Published in final edited form as:
Hypertension. 2010 April ; 55(4): 880–888. doi:10.1161/HYPERTENSIONAHA.109.145136.

Nebivolol Improves Diastolic Dysfunction and Myocardial Remodeling through Reductions in Oxidative Stress in the Zucker Obese Rat

Xinli Zhou[1,2,5], **Lixin Ma**[3,5], **Javad Habibi**[2,5], **Adam Whaley-Connell**[2,5], **Melvin R Hayden**[2], **Roger D Tilmon**[2], **Ashley N Brown**[3,5], **Jeong-a Kim**[2,5], **Vincent G. DeMarco**[2,4], and **James R Sowers**[2,4,5]

[1] Shandong Provincial Hospital Affiliated with Shandong University, Jinan, China

[2] University of Missouri School of Medicine, Department of Internal Medicine, Columbia, MO

[3] Department of Radiology, Columbia, MO

[4] Department of Medical Pharmacology and Physiology, Columbia, MO

[5] Harry S. Truman Veterans Affairs Medical Center, Columbia, MO

Abstract

Insulin resistance is associated with obesity and may be accompanied by left ventricular diastolic dysfunction and myocardial remodeling. Decreased insulin metabolic signaling and increased oxidative stress may promote these maladaptive changes. In this context, the β-blocker nebivolol has been reported to improve insulin sensitivity, increase eNOS activity, and reduce NADPH oxidase-induced superoxide generation. We hypothesized that nebivolol would attenuate diastolic dysfunction and myocardial remodeling by blunting myocardial oxidant stress and promoting insulin metabolic signaling in a rodent model of obesity, insulin resistance, and hypertension. Six week old male Zucker obese (ZO) and age-matched Zucker lean (ZL) rats were treated with nebivolol (10 $mg \cdot kg^{-1} \cdot day^{-1}$) for 21 days and myocardial function was assessed by cine magnetic resonance imaging. Compared to untreated ZL rats, untreated ZO rats exhibited prolonged diastolic relaxation time (27.7±2.5 vs 40.9±2.0 ms; $P<0.05$) and reduced initial diastolic filling rate (6.2±0.5 vs 2.8±0.6 μl/ms; $P<0.05$) in conjunction with increased HOMA-IR (7±2 vs 95±21; $P<0.05$), interstitial and pericapillary fibrosis, abnormal cardiomyocyte histoarchitecture, 3-nitrotyrosine, and NADPH oxidase-dependent superoxide. Nebivolol improved diastolic relaxation (32.8±0.7 ms; $P<0.05$ vs untreated ZO), reduced fibrosis and remodeling in ZO rats, in concert with reductions in nitrotyrosine, NADPH oxidase-dependent superoxide, and improvements in the insulin metabolic signaling, eNOS activation, and weight gain (381±7 vs 338±14 g; $P<0.05$). Results support the hypothesis that nebivolol reduces myocardial structural maladaptive changes and improves diastolic relaxation in concert with improvements in insulin sensitivity, and eNOS activation, concomitantly with reductions in oxidative stress.

Keywords

nebivolol; oxidative stress; insulin resistance; diastolic relaxation; MRI

Corresponding Author: James R. Sowers, MD, Professor of Medicine, and Medical Pharmacology and Physiology, Director of the Diabetes and Cardiovascular Center of Excellence, University of Missouri, One Hospital Drive, Columbia, MO 65212, Phone: (573) 882-2273; Fax: (573)884-5530 sowersj@health.missouri.edu.

Disclosures: JRS received Investigator Initiated Support from the Forest Research Institute.

Introduction

Obesity-induced cardiomyopathy is characterized by impaired left ventricular (LV) relaxation in association with insulin resistance (IR). [1,2] This cardiomyopathy develops independently of blood pressure, ischemia, impaired systolic function, and age.[1,2] Impaired insulin metabolic signaling and increased generation of reactive oxygen species (ROS) play an important role in maladaptive myocardial remodeling[3–5] and impaired diastolic relaxation. [6,7] Excessive ROS in the heart and vasculature, derived from several enzymatic sources, including nicotinamide adenine dinucleotide phosphate (NADPH) oxidase,[8] can lead to decreased bioavailable nitric oxide (NO) and reduced delivery of glucose and insulin to myocardial tissue.[4,9]

β-adrenergic receptor blockers have clinical utility in treating heart failure, but traditional β-blockers have been associated with weight gain, and worsening of IR.. Nebivolol, a third generation β_1-receptor blocker improves diastolic dysfunction[10] and reduces mortality in elderly heart failure patients.[10–12] Nebivolol does not have adverse effects on IR, nor does it cause weight gain. [13–15] Potential beneficial effects of nebivolol on diastolic dysfunction associated with IR may be mediated through improvements in bioavailable NO, reductions in ROS, and improvements in insulin metabolic signaling.

We hypothesized that nebivolol would improve diastolic dysfunction in an IR rat through reductions in NADPH oxidase activity and improved insulin metabolic signaling. To address our hypothesis, we utilized young (6–7 week old) Zucker obese (ZO) rats, an IR model which manifests increased myocardial oxidative stress and diastolic dysfunction.[16–18] Thus, the ZO rat provides a unique model to investigate the effect of nebivolol on impaired myocardial diastolic relaxation as a result of oxidative stress, reduced bioavailable NO, and impaired insulin metabolic signaling.[16]

Methods

Animals

Animal procedures were approved by the University of Missouri animal care committees and housed according to NIH guidelines.

Drug Preparation

Nebivolol was dissolved in 50% DMSO/50% propylene glycol to a final concentration of 70 mg/mL and filter sterilized. The solution (or its vehicle) was loaded into a model 2004 Alzet pump and inserted subcutaneously behind the shoulder blades under brief isoflurane anesthesia.

Systolic Blood Pressure and Total Body Weight

Within a day or two of termination of the experiment systolic blood pressures (SBPs) were measured in triplicate using the tail-cuff method as previously described.[19]

Homeostatic model assessment of Insulin Resistance (HOMA-IR)

A venous blood sample was collected from a subset of fasting rats in each treatment group at the end of the study and plasma was stored at −80°C. Glucose and insulin were measured by an automated hexokinase G-6-PDH assay and an ELISA kit specific for rat insulin, respectively. HOMA was calculated by taking the product of the glucose (mmol/L) and insulin (μU/mL) values and dividing by 22.

Cine-Magnetic Resonance Imaging

Magnetic resonance imaging (MRI) scans were performed on rats after 2 weeks treatment with nebivolol or vehicle. For details describing procedures to determine LV functional parameters please see http://hyper.ahajounals.org.

Light Microscopic Analysis for Myocardial Interstitial Fibrosis

Fixed paraffin sections of LV were evaluated with Verhoeff-van Gieson stain, which stains elastin (black), nuclei (blue black), collagen (pink), and connective tissue (yellow), as previously described.[19] For details of the morphometric analysis please see http://hyper.ahajounals.org.

Ultrastructural Analysis with Transmission electron microscopy (TEM)

Details of fixation, embedding, sectioning and staining procedures have been described previously.[19] A JOEL 1400-EX transmission electron microscope was used to view all samples.

Quantitative Analysis of Mitochondrial Number, Enzyme Level, and Activity

Mitochondrial quantification—Fixed samples were immunolabeled with an antibody to Complex IV-1 and viewed under a laser confocal microscope (Bio-Rad) and a multiphoton confocal system. Images were captured with Laser-sharp software and the immunofluorescence quantified using MetaMorph software. For details please see http://hyper.ahajounals.org.

Citrate Synthase Activity—Citrate synthase activity in mitochondrial fractions of LV tissue was determined as previously described.[20] For details please see http://hyper.ahajounals.org.

β-Hydroxyacyl-CoA dehydrogenase (β-HAD) activity—(β-HAD) activity was measured as previously described with modifications.[21] For details please see http://hyper.ahajounals.org.

Markers of Oxidative Stress

3-Nitrotyrosine immunostaining—3-nitrotyrosine was quantified as previously described.[19,22]

Superoxide formation—Superoxide was determined by chemiluminescense as previously described. [19,22] Superoxide values were normalized to total protein in the whole homogenate and expressed as relative light units per second per milligram of protein (RLU/s/mg).

NADPH oxidase activity—Activity was determined in plasma membrane fractions as previously described.[19,22]

Nox2, Nox4, Rac1, p47phox, eNOS, and Ser^{1177} eNOS Immunostaining—Left ventricular sections were immunostained, and quantitated as previously described.[19,22]

Quantification of IRS-1, Ser^{473} Akt, Ser^{1177}eNOS by Western Blot Analysis

Protein concentrations of tissue homogenates were measured as previously described.[19] Briefly, samples were separated by SDS-PAGE and transferred onto nitrocellulose membranes. Reactive bands were detected by chemiluminescence and images were recorded using a Bio-Rad ChemiDoc XRS image analysis system. Quantitation of protein band density, normalized

to β-actin band density, was performed using Quantity One software (Bio-Rad). Data are reported as normalized protein band density in arbitrary units.

Statistical Analysis

All values are expressed as means ± SE. Statistical analyses were performed with Sigma Stat (Aspire Software Intl, Ashburn, VA) using Student's *t* tests, or ANOVA with Fisher's least significant difference test for post-hoc comparisons. Significance was accepted as $P<0.05$.

Results

Nebivolol Effects on Body Weight and Systolic Blood Pressure (SBP)

Both the ZO-C and ZO-N groups had higher body weights compared to the ZL-C group (P<0.05) although there was a modest reduction in weight gain in the ZO-N rats compared to ZO-C rats (P<0.05) (Table 1). Although SBP tended to be higher in ZO-C and normalized in ZO-N compared to ZL-C rats the ANOVA main effect was not significant (P>0.05). A t-test indicated a significant decrease in SBP in ZO-N compared to ZO-C (128±5 vs 156±12 mmHg; P<0.05).

Nebivolol Effects on Insulin Resistance

ZO-C rats had elevated fasting plasma insulin levels (Table 1) compared to ZL-C (177±32 vs 21±5 μU/ml; P<0.05): nebivol treatment tended to blunt this hyperinsulinemia, but the trend was not significant (134±29 μU/ml; P>0.05 vs ZO-C). ZO-C rats were slightly hyperglycemic compared to ZL-C (11.4±1.2 vs 7.3±0.5 mM; P<0.05), although glucose levels were normalized in ZO-N (7.1±0.4μM; P<0.05 vs ZO-C). HOMA-IR indicated elevated IR in ZO-C compared to ZL-C (95±21 vs 7±2 mM; P<0.05), and ZO-N exhibited improved insulin sensitivity (41±8; P<0.05 vs ZO-C).

Nebivolol Improves Diastolic Relaxation

LV diastolic relaxation time, diastolic peak filling rate and initial filling rate, as well as septal wall thickness, ejection fraction, and stroke volume (SV) were determined via cine MRI (Figure 1A, B; Table 2). There were increases in septal wall thickness in ZO-C relative to ZL-C (P<0.05) and nebivolol tended to blunt the increased septal wall thickness in the ZO strain (P>0.05). LV diastolic relaxation time was prolonged in ZO-C compared with ZL-C (40.88 ±1.94 vs 27.68±2.50 mSec; P<0.05). Nebivolol decreased diastolic relaxation time in the ZO (ZO-N 32.77±0.73 mSec; P<0.05 vs ZO-C). Diastolic initial filling rate was reduced in ZO-C versus ZL-C (P<0.05). Heart rate, diastolic peak filling rate, systolic EF and SV were similar among all groups (Table 2).

Nebivolol Reduces Myocardial Interstitial Fibrosis

Interstitial fibrosis, as represented by the average gray scale intensity of VVG staining (for collagen), was increased in ZO-C compared with ZL-C (P<0.001), and improved in ZO-N compared with ZO-C (P<0.01) (Figure 1C). Coronary arterioles of ZO also exhibited perivascular fibrosis which was attenuated by nebivolol (not shown).

Nebivolol improves Myocardial Capillary and Tissue Remodeling

On ultrastructural analysis there were constricted capillaries with pericapillary fibrosis in the ZO-C myocardium which improved with nebivolol treatment (Figure 1D). There was also an increase in endothelial cell transcytotic vesicles in ZO-N rats compared to ZO-C (Figure 1D).

Nebivolol Improves Mitochondrial Function and Structure

Mitochondrial Complex IV subunit 1, the last enzyme in the respiratory electron transport chain and an index of mitochondrial number, was quantitated by protein immunofluorescence. Citrate synthase, a Kreb's cycle enzyme used to assess aerobic capacity of mitochondria, and β-HAD, an enzyme involved in mitochondrial fatty acid β-oxidation were also quantitated. Control ZO myocardium exhibited increased ($P<0.05$) mitochondrial numbers (increase in Complex IV-1), without differences in citrate synthase and β-HAD (Figure 2A, B, and C, respectively). Complex IV-1 signal in the ZO myocardium was reduced with nebivolol treatment ($P<0.05$). Normal levels of citrate synthase and β-HAD activities, coupled with the increased numbers of mitochondria in the ZO myocardium, suggest that it takes more mitochondria in the ZO myocardium to provide normal levels of ATP. Nebivolol treatment restored the enzyme activities and mitochondrial number in ZO to levels similar to those in the ZL-C and ZL-N myocardium. Compared with ZL-C, ZL-N, and ZO-N, ZO-C demonstrated increases in intermyofibrillar mitochondria and disorganized sarcomere structure (Figure 2D). ZO-C mitochondria exhibited swollen and disrupted cristae (Figure 2E). Nebivolol abrogated the increased mitochondrial biogenesis and improved mitochondrial sarcomere organization (Figure 2D and E).

Nebivolol Reduces Myocardial NADPH Oxidase Activity

NADPH oxidase activity was elevated in ZO-C compared to that of ZL-C ($P<0.05$; Figure 3A). ZO-N had lower NADPH oxidase activity vs ZO-C rats ($P<0.05$). There were also increases in NADPH oxidase subunit immunostaining of Nox2, Nox4, Rac1 and $p47^{phox}$ in ZO-C compared with ZL-C ($P<0.05$ for each; Figure 3C). Expression levels for all of these proteins were normalized following nebivolol therapy ($P<0.05$ vs ZO-C for each protein).

Nebivolol Reduces Myocardial Oxidative Stress

There were increases in superoxide levels in ZO myocardium compared with ZL ($P<0.05$; Figure 3B). ZO-N rats had lower superoxide levels compared to ZO-C rats ($P<0.05$). There were increases in myocardial 3-nitrotyrosine (3-NT) content in the ZO-C (32.8±2.1 grayscale intensities) compared with ZL-C (19.2 ± 2.1; $P<0.05$) and 3-NT was reduced in nebivolol treated ZO rats (22.1±2.1; $P<0.05$; Figure 3D).

Nebivolol modulates the IRS-1/Akt/eNOS Signaling Pathway

To explore whether nebivolol modulates myocardial insulin signaling, we examined the IRS-1/Akt/eNOS cascade by immunoblotting (Figure 4A–C). Although the protein levels of IRS-1 or the ratio of phosphorylated Akt at Ser^{473} to total Akt were similar in the ZL-C, ZL-N and ZO-C groups, there was a 2.26-fold increase in IRS-1 content and a 2.05-fold increase in activated Akt, i.e., the ratio of phosphorylated Akt at Ser^{473} to total Akt, in ZO rats treated with nebivolol compared with ZO controls (each $P<0.05$; Figure 4A, B).

To ascertain whether nebivolol induced eNOS activation in ZO heart tissue, Ser^{1177} phosphorylation of eNOS (activation) and total eNOS protein were measured using western blots (Figure 4C). There were increases in Ser^{1177} eNOS (1.79-fold) and eNOS (1.59-fold) in ZO rats with nebivolol treatment compared with ZO controls (each $P<0.05$). The ratio of Ser^{1177} eNOS to total eNOS in the ZO-C was not different from ZL-C ($P>0.05$); however, the ratio of Ser^{1177} eNOS to total eNOS was increased in ZO-N compared to ZO-C ($P<0.01$).

To more specifically evaluate myocardial or coronary arteriolar changes in total eNOS and phosphorylated eNOS at Ser^{1177} we performed semi-quantitative immunofluorescence analyses. Both total eNOS and Ser^{1177} eNOS immunofluorescent signals were detected in the

myocardium and in the vascular wall of coronary arterioles (Figure 4D). Ser^{1177}eNOS was increased in ZO rats treated with nebivolol compared to ZO controls (Figure 4D; $P<0.05$).

Discussion

This investigation demonstrates that nebivolol improves LV diastolic function and insulin sensitivity, reduces myocardial NADPH oxidase activity, oxidative stress, and interstitial fibrosis, reduces capillary and mitochondria ultrastructural abnormalities, and enhances the IRS-1/Akt/eNOS signaling pathway. Finally, nebivolol, unlike traditional β-blockers which promote weight gain,[23] reduced weight gain in the ZO rat.

In metabolic heart disease, relaxation abnormalities often appear prior to the onset of contractile dysfunction. Diastolic dysfunction is characterized by a decrease in the ability of the LV to fill with blood during the early diastolic filling.[24] Using high-resolution cine-MRI we observed delayed LV diastolic relaxation and decreased early diastolic filling in the ZO rat in the absence of measurable contractile dysfunction. Nebivolol treatment improved LV diastolic relaxation, in concert with reductions in interstitial fibrosis.

There were substantive ultrastructural abnormalities of the coronary microvasculature and intermyofibrillar mitochondria in ZO hearts which were reversed with nebivolol treatment. Capillaries were constricted, exhibited diffuse pericapillary fibrosis, and contained fewer transcytotic vesicles in endothelial cells. ZO hearts had marked increases in intermyofibrillar mitochondria which resulted in disorganized sarcomere structure as previously observed in other rodent models of IR.[19,25–27] The increase in Complex IV-1 in ZO-C, while indicative of an increase in number of mitochondria, may also reflect a compensatory response which limits oxidative stress by diverting molecular oxygen toward the terminal steps in aerobic metabolism leading to ATP synthesis. Indeed, there is recent evidence that mitochondria in the untreated diabetic ZO heart produce excessive superoxide.[28] There was a marked reduction in mitochondria in nebivolol treated ZO hearts, yet they exhibited improved cristae structure and sarcomere organization.

The balance between ROS production and elimination plays a key role in preserving cardiac function; excessive myocardial ROS precipitates impairment of myocardial function and abnormalities in cardiac structure.[29] The NADPH oxidase complex, serves as a major source for generation of superoxide in the cardiovascular system. ZO myocardium had increases in NADPH oxidase activity, superoxide, and 3-NT; these increases were blunted with nebivolol therapy. There were increases in NADPH subunits Nox2, Nox4, $p47^{phox}$ and Rac1 in ZO-C hearts; however, the expression of all these proteins was significantly reduced by nebivolol treatment. These data suggest that NADPH oxidase activation may be the primary mediator of increased superoxide production in the heart of ZO rat. In diabetic fatty rats the mitochondria may also be a significant source of ROS in the myocardium.[28] Interestingly, these young ZO rats did not exhibit increases in mitochondrial citrate synthase activity, or β-HAD, a marker of fatty acid β-oxidation. Excessive fatty acid oxidation can lead to increased mitochondrial superoxide synthesis. Others have shown increased fatty acid uptake in ZO hearts[30,31] in the absence of increased fatty acid oxidation.[32]

IR is associated with endothelial dysfunction and impaired vasodilation which may be partially dependent on excess generation of ROS.[4,33] Superoxide may react with NO released by eNOS to generate peroxynitrite. The increased 3-NT staining in the ZO myocardium observed in this study is indirect evidence of formation of peroxynitrite. Peroxynitrite can contribute to endothelial dysfunction by reducing the bioavailability of NO, [33,34] in part, by promoting uncoupling of eNOS which results in eNOS-derived increases in superoxide synthesis.[4]

eNOS activity is regulated by posttranslational modifications including phosphorylation of specific sites and protein-protein interactions. Phosphorylation of eNOS at Ser^{1177} is associated with increased enzyme activity.[3] The ZO rat exhibits impairments in endothelial function and endothelium-dependent vasodilation.[35] In this study, both eNOS expression and eNOS phosphorylation at Ser^{1177} were increased in coronary arterioles of ZO rats with nebivolol treatment. Commensurate with these changes in eNOS, TEM measurements demonstrated constricted capillaries with decreased endothelial transcytotic vesicles in ZO rats that improved with nebivolol treatment. Our data suggests that nebivolol improves capillary endothelial function and remodeling in the ZO rat and that this may be due to a reduction in oxidative stress, promotion of nitric oxide bioavailability, and an increase in NO biosynthesis. This compliments a prior observation that nevivolol inhibits endothelial dysfunction via diminishing superoxide formation by NADPH oxidase in the heart of angiotension II-treated rats.[36] In the heart, among the three isoforms of NOS, eNOS is constitutively expressed in both endothelial cells and cardiomyocytes[37]. NO produced by eNOS is not only a primary determinant of blood vessel tone, but also a regulator of cardiac function. In this regard, eNOS-derived NO facilitates increased myocardial diastolic relaxation and decreased O_2 consumption.[38]

Activation of the IRS-1/Akt pathway plays a central role in the regulation of myocardial glucose metabolism, cell survival and cardiac function.[19] In particular, the IRS-1/Akt pathway activates eNOS by phosphorylation at the $Serine^{1177}$ residue which promotes NO production.[39] Our laboratory has previously observed that there was a relationship between increased NADPH oxidase activity and diminished Akt activation in vivo.[3,19] In this study, there were significant increases in phosphorylated Ser^{473} Akt as well as total IRS-1 protein in ZO rats with nebivolol treatment in the absence of significant differences in the expression of IRS-1, Akt phosphorylation, eNOS as well as eNOS phosphorylation between control ZO and ZL rats at 9 weeks of age. This somewhat surprising result suggests there could be a compensatory mechanism under hyperinsulinemia in the young ZO rats. Despite the apparent normal state of eNOS activation in the untreated ZO myocardium observed in this study, it is likely that nebivolol acts to enhance the bioavailability of NO by reducing levels of ROS and promoting activation of the IRS-1/Akt/eNOS pathway. Indeed, nebivolol dilates the coronary arterial microvasculature via an agonist effect on endothelial β_3-adrenoreceptors that promotes release of NO, in part, by dephosphorylating eNOS on Thr^{495}.[40] Such a scenario predicts improvements in cardiac function and structure.

The notion that traditional β-blockers, promote modest weight gain may be due to several factors including reductions in metabolic rate and insulin sensitivity.[23,41] However, our data suggests that nebivolol treated ZO rats, on average, weighed less by 11% ($P<0.05$), were more insulin sensitive, and normotensive compared to control ZO rats. This is consistent with observations in human trials wherein nebivolol has largely been found to be weight and metabolically neutral compared to more traditional agents.[14,15] However, it is possible this modest weight loss contributes to the overall improvements in insulin sensitivity, systolic blood pressure, and diastolic function. In obese humans, modest weight loss can lead to improvements in insulin sensitivity, decreased blood pressure, and improved endothelial function. It is also possible that the β3 agonist properties of nebivolol mediate modest weight loss by inducing trans-differentiation of white adipose tissue into brown adipose tissue.[42] Indeed, in rodents and humans β3 receptor agonists stimulate oxidation of fats, reduce fat weight, improve insulin sensitivity, and spare lean body mass.[43]

Perspectives

This investigation indicates that nebivolol, a highly cardioselective β_1-receptor blocker, improves myocardial remodeling and diastolic dysfunction as well as IRS-1/Akt/eNOS signaling pathways by inhibiting myocardial NADPH oxidase-mediated superoxide formation

in an obese insulin resistant rodent model. These findings suggest that nebivolol prevents or at least delays the development of cardiomyopathy associated with insulin resistance. Finally, nebivolol, unlike traditional β-blockers which promote weight gain, reduced weight gain in the ZO rat. These data are highly clinically relevant as a first report using an animal model of obesity that ascribes potential mechanisms to explain observed human improvements in diastolic function and insulin sensitivity in patients on nebivolol.

Supplementary Material

Refer to Web version on PubMed Central for supplementary material.

Acknowledgments

Exceptional support was provided by the VA Biomolecular Imaging Center at the Harry S Truman VA Hospital, as well as the Electron Microscope Core Center at the University of Missouri-Columbia for their help with tissue preparation of animal specimens.

Sources of Funding: This research was supported by NIH (R01 HL73101-01A1) to JRS, and Veterans Affairs Merit System (0018) for JRS and CDA-2 and VISN15 for AWC, and the Forest Research Institute.

References

1. Alpert MA, Lambert CR, Terry BE, Cohen MV, Mukerji V, Massey CV, Hashimi MW, Panayiotou H. Interrelationship of left ventricular mass, systolic function and diastolic filling in normotensive morbidly obese patients. Int J Obes Relat Metab Disord 1995;19:550–557. [PubMed: 7489025]
2. Lauer MS, Anderson KM, Kannel WB, Levy D. The impact of obesity on left ventricular mass and geometry. The Framingham Heart Study. JAMA 1991;266:231–236. [PubMed: 1829117]
3. Wei Y, Whaley-Connell AT, Chen K, Habibi J, Uptergrove GM, Clark SE, Stump CS, Ferrario CM, Sowers JR. NADPH oxidase contributes to vascular inflammation, insulin resistance, and remodeling in the transgenic (mRen2) rat. Hypertension 2007;50:384–391. [PubMed: 17533199]
4. Munzel T, Daiber A, Ullrich V, Mulsch A. Vascular consequences of endothelial nitric oxide synthase uncoupling for the activity and expression of the soluble guanylyl cyclase and the cGMP-dependent protein kinase. Arterioscler Thromb Vasc Biol 2005;25:1551–1557. [PubMed: 15879305]
5. Cai H, Harrison DG. Endothelial dysfunction in cardiovascular diseases: the role of oxidant stress. Circ Res 2000;87:840–844. [PubMed: 11073878]
6. Sawyer DB, Siwik DA, Xiao L, Pimentel DR, Singh K, Colucci WS. Role of oxidative stress in myocardial hypertrophy and failure. J Mol Cell Cardiol 2002;34:379–388. [PubMed: 11991728]
7. Sorescu D, Griendling KK. Reactive oxygen species, mitochondria, and NAD(P)H oxidases in the development and progression of heart failure. Congest Heart Fail 2002;8:132–140. [PubMed: 12045381]
8. Griendling KK, Ushio-Fukai M. Reactive oxygen species as mediators of angiotensin II signaling. Regul Pept 2000;91:21–27. [PubMed: 10967199]
9. Takimoto E, Kass DA. Role of oxidative stress in cardiac hypertrophy and remodeling. Hypertension 2007;49:241–248. [PubMed: 17190878]
10. Nodari S, Metra M, Dei CL. Beta-blocker treatment of patients with diastolic heart failure and arterial hypertension. A prospective, randomized, comparison of the long-term effects of atenolol vs. nebivolol. Eur J Heart Fail 2003;5:621–627. [PubMed: 14607201]
11. Ghio S, Magrini G, Serio A, Klersy C, Fucili A, Ronaszeki A, Karpati P, Mordenti G, Capriati A, Poole-Wilson PA, Tavazzi L. Effects of nebivolol in elderly heart failure patients with or without systolic left ventricular dysfunction: results of the SENIORS echocardiographic substudy. Eur Heart J 2006;27:562–568. [PubMed: 16443607]
12. van Veldhuisen DJ, Cohen-Solal A, Bohm M, Anker SD, Babalis D, Roughton M, Coats AJ, Poole-Wilson PA, Flather MD. Beta-blockade with nebivolol in elderly heart failure patients with impaired and preserved left ventricular ejection fraction: Data From SENIORS (Study of Effects of Nebivolol

Intervention on Outcomes and Rehospitalization in Seniors With Heart Failure). J Am Coll Cardiol 2009;53:2150–2158. [PubMed: 19497441]

13. Manrique C, Whaley-Connell A, Sowers JR. Nebivolol in obese and non-obese hypertensive patients. J Clin Hypertens (Greenwich) 2009;11:309–315. [PubMed: 19527321]
14. Celik T, Iyisoy A, Kursaklioglu H, Kardesoglu E, Kilic S, Turhan H, Yilmaz MI, Ozcan O, Yaman H, Isik E, Fici F. Comparative effects of nebivolol and metoprolol on oxidative stress, insulin resistance, plasma adiponectin and soluble P-selectin levels in hypertensive patients. J Hypertens 2006;24:591–596. [PubMed: 16467663]
15. Rizos E, Bairaktari E, Kostoula A, Hasiotis G, Achimastos A, Ganotakis E, Elisaf M, Mikhailidis DP. The combination of nebivolol plus pravastatin is associated with a more beneficial metabolic profile compared to that of atenolol plus pravastatin in hypertensive patients with dyslipidemia: a pilot study. J Cardiovasc Pharmacol Ther 2003;8:127–134. [PubMed: 12808486]
16. Kurtz TW, Morris RC, Pershadsingh HA. The Zucker fatty rat as a genetic model of obesity and hypertension. Hypertension 1989;13:896–901. [PubMed: 2786848]
17. Poornima IG, Parikh P, Shannon RP. Diabetic cardiomyopathy: the search for a unifying hypothesis. Circ Res 2006;98:596–605. [PubMed: 16543510]
18. Vincent HK, Powers SK, Stewart DJ, Shanely RA, Demirel H, Naito H. Obesity is associated with increased myocardial oxidative stress. Int J Obes Relat Metab Disord 1999;23:67–74. [PubMed: 10094579]
19. Whaley-Connell A, Govindarajan G, Habibi J, Hayden MR, Cooper SA, Wei Y, Ma L, Qazi M, Link D, Karuparthi PR, Stump CS, Ferrario CM, Sowers JR. Angiotensin-II mediated oxidative stress promotes myocardial tissue remodeling in the transgenic TG (mRen2) 27 Ren2 rat. Am J Physiol Endocrinol Metab 2007;293:E355–E363. [PubMed: 17440033]
20. Srere PA. Citrate Synthase. Methods Enzymol 1969:3–5.
21. Bass A, Brdiczka D, Eyer P, Hofer S, Pette D. Metabolic differentiation of distinct muscle types at the level of enzymatic organization. Eur J Biochem 1969;10:198–206. [PubMed: 4309865]
22. Whaley-Connell A, Habibi J, Cooper SA, DeMarco VG, Hayden MR, Stump CS, Link D, Ferrario C, Sowers JR. Effect of Renin Inhibition and AT1R Blockade on Myocardial Remodeling in the Transgenic Ren2 Rat. Am J Physiol Endocrinol Metab 2008;295:E103–E109. [PubMed: 18460596]
23. Messerli FH, Bell DS, Fonseca V, Katholi RE, McGill JB, Phillips RA, Raskin P, Wright JT Jr, Bangalore S, Holdbrook FK, Lukas MA, Anderson KM, Bakris GL. Body weight changes with beta-blocker use: results from GEMINI. Am J Med 2007;120:610–615. [PubMed: 17602935]
24. Nishimura RA, Tajik AJ. Evaluation of diastolic filling of left ventricle in health and disease: Doppler echocardiography is the clinician's Rosetta Stone. J Am Coll Cardiol 1997;30:8–18. [PubMed: 9207615]
25. Nishio Y, Kanazawa A, Nagai Y, Inagaki H, Kashiwagi A. Regulation and role of the mitochondrial transcription factor in the diabetic rat heart. Ann N Y Acad Sci 2004;1011:78–85. [PubMed: 15126286]
26. Duncan JG, Fong JL, Medeiros DM, Finck BN, Kelly DP. Insulin-resistant heart exhibits a mitochondrial biogenic response driven by the peroxisome proliferator-activated receptor-alpha/PGC-1alpha gene regulatory pathway. Circulation 2007;115:909–917. [PubMed: 17261654]
27. Stas S, Whaley-Connell A, Habibi J, Appesh L, Hayden MR, Karuparthi PR, Qazi M, Morris EM, Cooper SA, Link CD, Stump C, Hay M, Ferrario C, Sowers JR. Mineralocorticoid receptor blockade attenuates chronic overexpression of the renin-angiotensin-aldosterone system stimulation of NADPH oxidase and cardiac remodeling. Endocrinology 2007;148:3773–3780. [PubMed: 17494996]
28. Serpillon S, Floyd BC, Gupte RS, George S, Kozicky M, Neito V, Recchia F, Stanley W, Wolin MS, Gupte SA. Superoxide production by NAD(P)H oxidase and mitochondria is increased in genetically obese and hyperglycemic rat heart and aorta before the development of cardiac dysfunction. The role of glucose-6-phosphate dehydrogenase-derived NADPH. Am J Physiol Heart Circ Physiol 2009;297:H153–H162. [PubMed: 19429815]
29. Ritchie RH, Delbridge LM. Cardiac hypertrophy, substrate utilization and metabolic remodelling: cause or effect? Clin Exp Pharmacol Physiol 2006;33:159–166. [PubMed: 16445716]

30. Luiken JJ, Arumugam Y, Dyck DJ, Bell RC, Pelsers MM, Turcotte LP, Tandon NN, Glatz JF, Bonen A. Increased rates of fatty acid uptake and plasmalemmal fatty acid transporters in obese Zucker rats. J Biol Chem 2001;276:40567–40573. [PubMed: 11504711]

31. Coort SL, Hasselbaink DM, Koonen DP, Willems J, Coumans WA, Chabowski A, Van d V, Bonen A, Glatz JF, Luiken JJ. Enhanced sarcolemmal FAT/CD36 content and triacylglycerol storage in cardiac myocytes from obese zucker rats. Diabetes 2004;53:1655–1663. [PubMed: 15220187]

32. Young ME, Guthrie PH, Razeghi P, Leighton B, Abbasi S, Patil S, Youker KA, Taegtmeyer H. Impaired long-chain fatty acid oxidation and contractile dysfunction in the obese Zucker rat heart. Diabetes 2002;51:2587–2595. [PubMed: 12145175]

33. Katakam PV, Tulbert CD, Snipes JA, Erdos B, Miller AW, Busija DW. Impaired insulin-induced vasodilation in small coronary arteries of Zucker obese rats is mediated by reactive oxygen species. Am J Physiol Heart Circ Physiol 2005;288:H854–H860. [PubMed: 15650157]

34. Laight DW, Anggard EE, Carrier MJ. Investigation of basal endothelial function in the obese Zucker rat in vitro. Gen Pharmacol 2000;35:303–309. [PubMed: 11922960]

35. Russo I, Del MP, Doronzo G, Mattiello L, Viretto M, Bosia A, Anfossi G, Trovati M. Resistance to the nitric oxide/cyclic guanosine 5′-monophosphate/protein kinase G pathway in vascular smooth muscle cells from the obese Zucker rat, a classical animal model of insulin resistance: role of oxidative stress. Endocrinology 2008;149:1480–1489. [PubMed: 18079207]

36. Oelze M, Daiber A, Brandes RP, Hortmann M, Wenzel P, Hink U, Schulz E, Mollnau H, von SA, Kleschyov AL, Mulsch A, Li H, Forstermann U, Munzel T. Nebivolol inhibits superoxide formation by NADPH oxidase and endothelial dysfunction in angiotensin II-treated rats. Hypertension 2006;48:677–684. [PubMed: 16940222]

37. Massion PB, Dessy C, Desjardins F, Pelat M, Havaux X, Belge C, Moulin P, Guiot Y, Feron O, Janssens S, Balligand JL. Cardiomyocyte-restricted overexpression of endothelial nitric oxide synthase (NOS3) attenuates beta-adrenergic stimulation and reinforces vagal inhibition of cardiac contraction. Circulation 2004;110:2666–2672. [PubMed: 15492314]

38. Massion PB, Feron O, Dessy C, Balligand JL. Nitric oxide and cardiac function: ten years after, and continuing. Circ Res 2003;93:388–398. [PubMed: 12958142]

39. Kadi A, Moby V, de IN, Lacolley P, Menu P, Stoltz JF. Signalling transduction pathways implicated in Nebivolol-induced NO production in endothelial cells. Biomed Mater Eng 2008;18:303–307. [PubMed: 19065039]

40. Dessy C, Saliez J, Ghisdal P, Daneau G, Lobysheva II, Frerart F, Belge C, Jnaoui K, Noirhomme P, Feron O, Balligand JL. Endothelial beta3-adrenoreceptors mediate nitric oxide-dependent vasorelaxation of coronary microvessels in response to the third-generation beta-blocker nebivolol. Circulation 2005;112:1198–1205. [PubMed: 16116070]

41. Manrique C, Johnson M, Sowers JR. Thiazide diuretics alone or with beta-blockers impair glucose metabolism in hypertensive patients with abdominal obesity. Hypertension 2010;55:15–17. [PubMed: 19917873]

42. Solak Y, Atalay H. Nebivolol in the treatment of metabolic syndrome: Making the fat more brownish. Med Hypotheses. 2009 epub ahead of print.

43. Arch JR. The discovery of drugs for obesity, the metabolic effects of leptin and variable receptor pharmacology: perspectives from beta3-adrenoceptor agonists. Naunyn Schmiedebergs Arch Pharmacol 2008;378:225–240. [PubMed: 18612674]

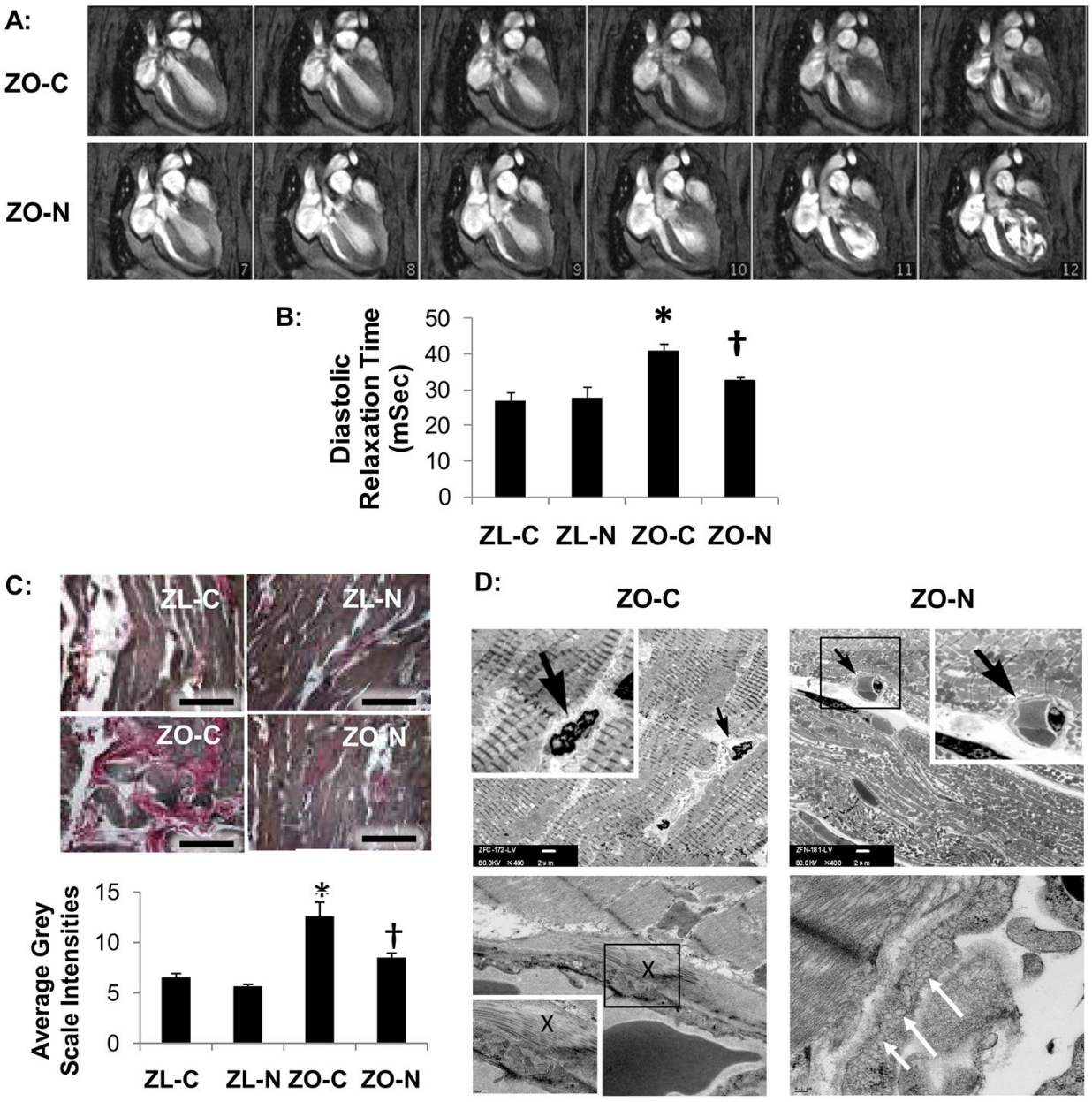

Figure 1. Nebivolol improves diastolic relaxation, reduces myocardial fibrosis, and improves ultrastructural remodeling of myocardial capillaries

A, Representative cine-MRI images illustrate early diastole phases (frame 7–12 of 16 captured) in a cardiac cycle. The upper row demonstrates prolonged diastolic relaxation time in ZO-C compared to reduced diastolic relaxation time and increased initial filling rate in ZO-N shown in the lower row. B, Bar graph shows diastolic relaxation times for experimental groups. C, Light micrographs show representative LV sections stained with Verhoeff-van Gieson stain, which stains collagen pink. The bar graph below shows that nebivolol attenuates the increased interstitial fibrosis in the ZO myocardium. Scale bar=50 μm. *P<0.001 vs ZL-C; †P<0.01 vs ZO-C. D, Representative TEM micrographs at ×400 demonstrate constricted capillaries in ZO-C that improved with nebivolol treatment in ZO-N (upper panels). Small dark arrows point to a capillaris which are shown at higher magnification in the white boxes. Scale bar = 2μm. The

X in the center of the lower left panel shows pericapillary fibrosis in the ZO-C heart and the area inside the dark box is shown at higher magnification in the white box (scale bar=0.1 μm). From bottom to top, each image shows the capillary lumen, a single endothelial cell layer comprising the capillary wall, a prominent layer of pericapillary collagen, and cardiomyocytes. A pericapillary collagen layer was not observed in the ZO-N (lower right panel). White arrows indicate an area of abundant endothelial cell transcytotic vesicles in the ZO-N.

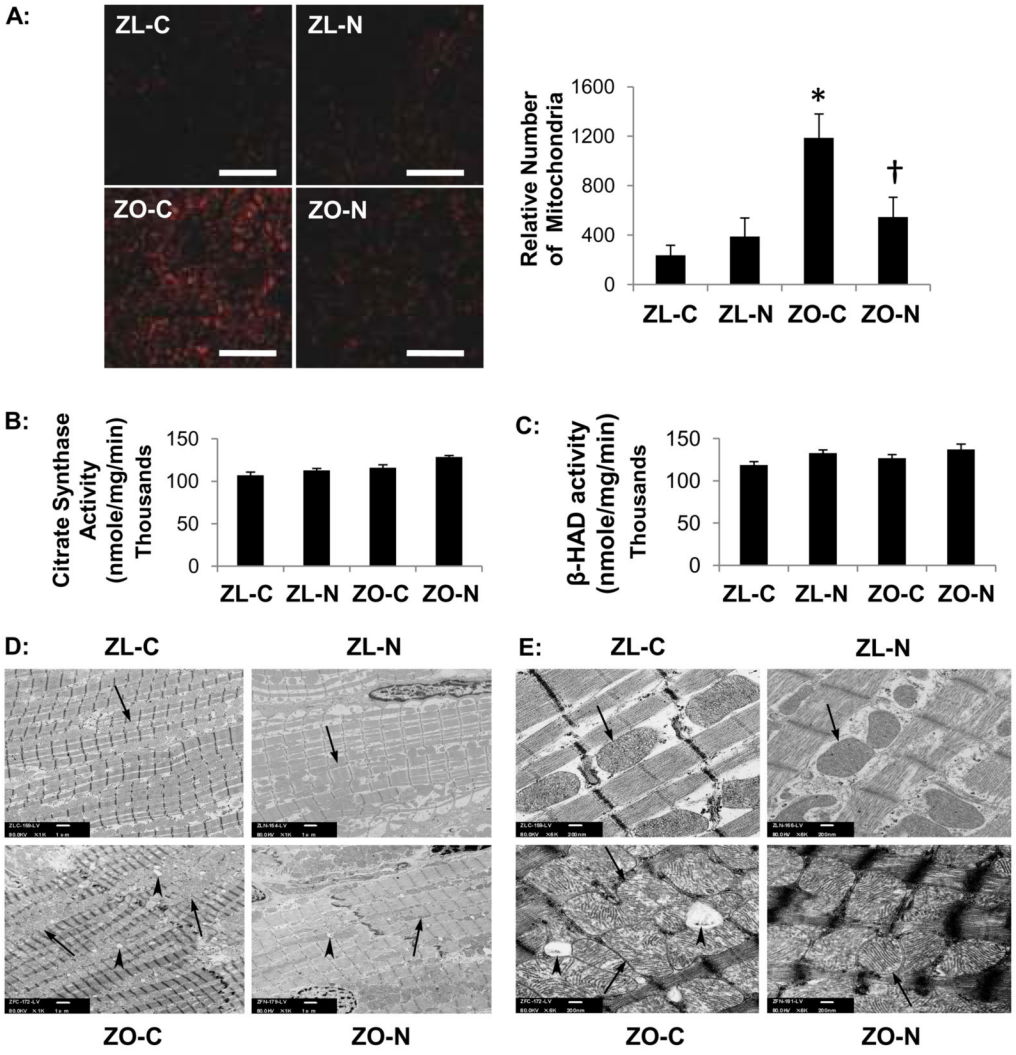

Figure 2. Nebivolol improves myocardial mitochondrial function

A, Representative left ventricular sections immunostained for mitochondrial Complex IV-1 of treated and untreated ZL and ZO rats. The increased level of Complex IV-1 immunostaining in the ZO-C myocardium indicates increased mitochondrial number compared to all other groups. Bar graph to the right shows quantification of converted signal intensities of Complex IV-1 protein. B, Bar graphs show myocardial citrate synthase and C, β-HAD activities. No differences were observed in enzyme activities among the groups ($P>0.05$). *$P<0.05$ vs ZL-C; †$P<0.05$ vs ZO-C. D, Representative myocardial TEM micrographs at ×1,000. Compared to ZL-C (upper left) ZO-C rats possess increased numbers of intermyofibrillar mitochondrial and a disorganized sarcomere structure (lower left). An abrogation of the increased mitochondrial biogenesis was observed in ZO-N rats (lower right). Scale bar=1 μm. E, Representative TEM micrographs show intermyofibrillar mitochondria at ×6,000. Compared to ZL-C (upper left) the ZO-C myocardium (lower left) shows multiple layers of mitochondria between myofibrils compared to a single layer arrangement of mitochondria in ZL-C, ZL-N and ZO-N hearts. Large lipid droplets are more abundant in the ZO-C myocardium which also shows abnormal mitochondrial structure (swollen and disrupted cristae and irregular open matrix). The appearance of mitochondria was improved in the ZO-N myocardium (lower right). Scale bar=200nm. Arrows point to mitochondria and arrowheads point to lipid droplets.

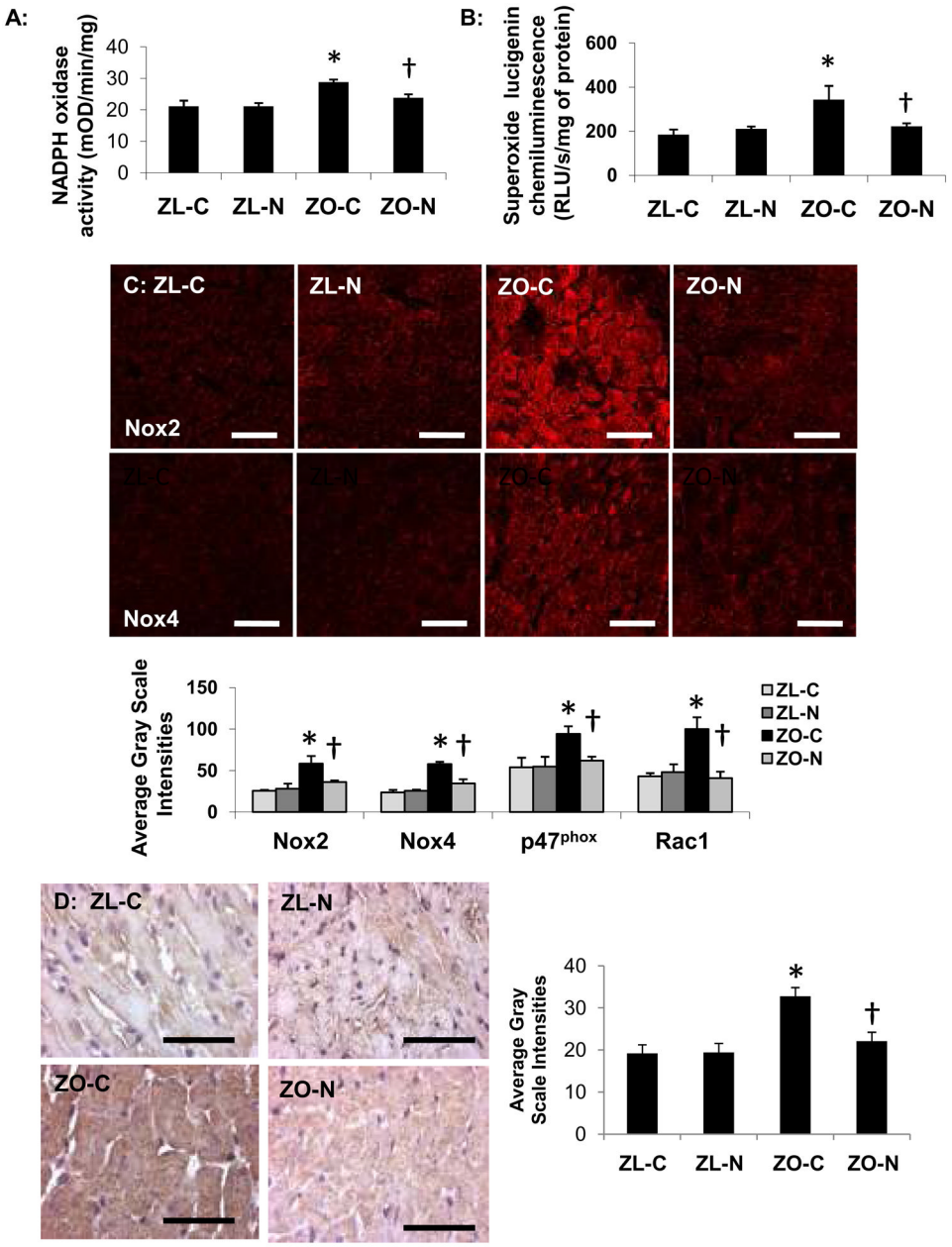

Figure 3. Nebivolol reduces NADPH oxidase subunit protein expression

A, The bar graph demonstrates increased NADPH oxidase activity in the myocardium of ZO-C relative to ZL-C ($P<0.05$). Nebivolol reduces NADPH oxidase activity in the ZO myocardium compared to ZO-C ($P<0.05$). B, The bar graph demonstrates increased formation of superoxide in the myocardium of ZO-C relative to ZL-C ($P<0.05$). Nebivolol reduces superoxide formation in the ZO myocardium compared to ZO-C ($P<0.05$). C, Representative confocal images showing immunofluorescence for NADPH oxidase membrane bound proteins Nox2 and Nox4. B, Bar graphs show average gray scale intensities for NADPH oxidase subunits Nox2, Nox4, $p47^{phox}$ and Rac1 as. D Representative photomicrographs showing 3-nitrotyrosine immunostaining in the myocardium of ZL and ZO rats. In the bar graph to the right average grayscale intensity measures of the 3-nitrotyrosine staining show that nebivolol

blunts the increase in 3-nitrotyrosine levels in the ZO myocardium. Scale bar=50μm. *P<0.05 vs ZL-C; †P<0.05 vs ZO-C.

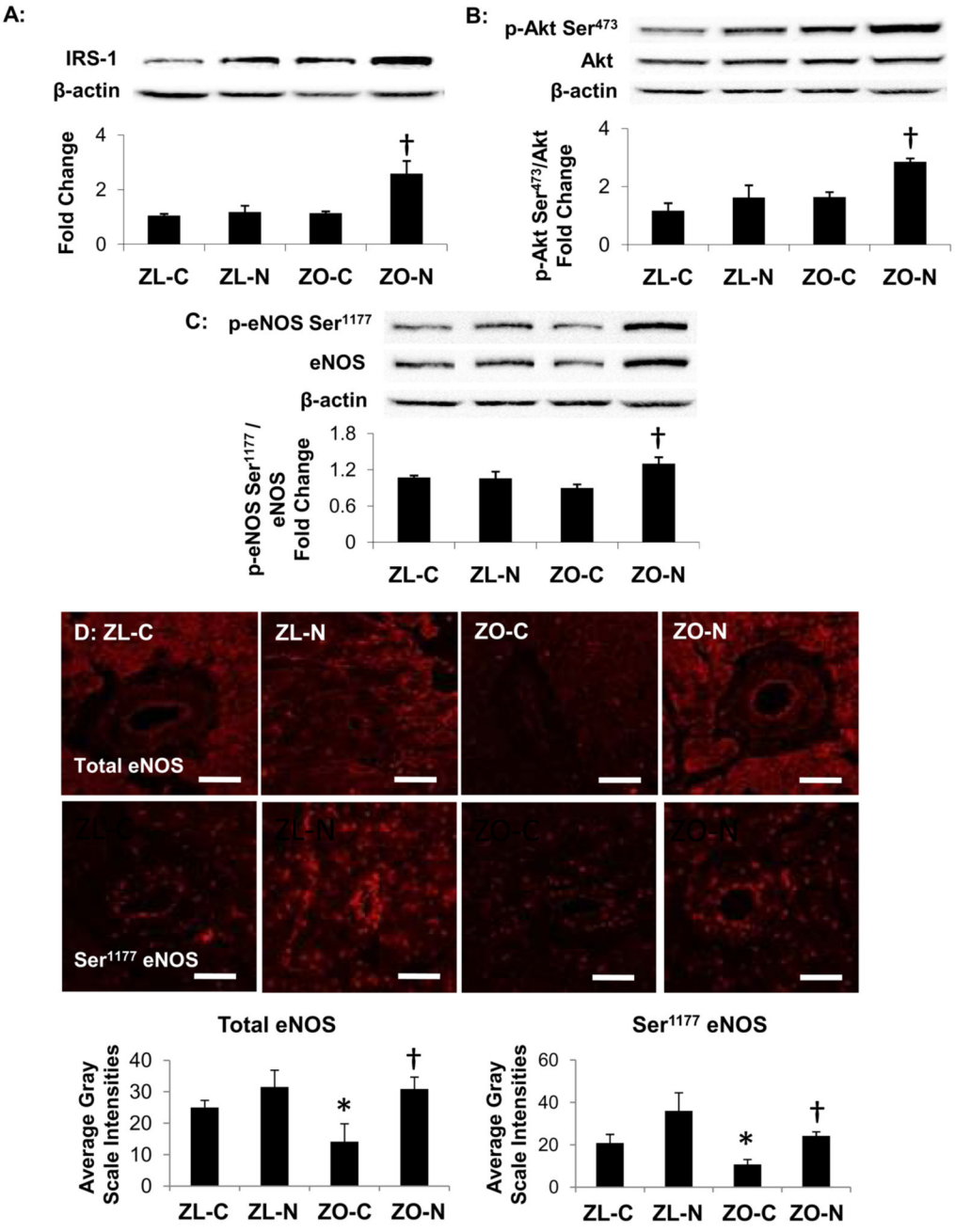

Figure 4. Nebivolol improves insulin metabolic signaling and enhances coronary arteriolar eNOS activation

A, The bar graph shows a quantitative densitometric analysis for IRS-1 protein (normalized to β-actin) as a percentage of ZL-C (i.e., fold increase). Representative protein bands for IRS-1 and β-actin are shown above the bar graph. Nebivolol increased IRS-1 protein level in the ZO myocardium compared to ZO-C. B, Representative western blots show phosphorylated Ser^{473} Akt and total Akt, as well as their corresponding β-actin bands. The bar graph shows the ratio of phospho-Akt to total Akt expressed as a percentage of ZL-C control. C, Representative western blots show phosphorylated eNOS at Ser^{1177} and total eNOS, as well as their corresponding β-actin bands. The bar graph displays the ratio of phospho-eNOS Ser^{1177} to total eNOS expressed as a percentage of ZL-C control. D, Representative confocal

micrographs show total eNOS (upper row) and phospho-eNOS Ser^{1177} (lower row) immunofluorescence in the myocardium and coronary arterioles of ZL and ZO rats. Scale bar=50 μm. The bar graphs below show average grayscale intensity measures of total eNOS (left) and phospho-eNOS Ser^{1177} (right) immunofluorescence in the endothelium of coronary arterioles of ZL and ZO rats and indicate that nebivolol enhances eNOS phosphorylation at serine^{1177} *P<0.05 vs ZL-C; †P<0.05 vs ZO-C.

Table 1

Effects of nebivolol on body weight, blood pressure, fasting plasma glucose and insulin, and insulin sensitivity (HOMA-IR) of 9 week old ZL and ZO rats. Numbers in parentheses are sample sizes.

Parameter	ZL-C	ZL-N	ZO-C	ZO-N
Body Weight (g)	245 ± 7 (6)	240 ± 7 (6)	381 ± 7(6)*	338 ± 14 (6)*†
SBP (mmHg)	136 ± 11 (5)	133 ± 10 (6)	156 ± 12 (6)	128 ± 5 (7)
Glucose (mmoles/L)	7.3 ± 0.5 (6)	6.6 ± 0.6 (2)	11.4 ± 1.2 (8) *	7.1 ± 0.4 (6)†
Insulin (μU/ml)	21 ± 5 (6)	18 ± 12 (2)	177 ± 32 (8) *	134 ± 29 (6)
HOMA-IR	7.2 ± 1.9 (6)	5.6 ± 4.1 (2)	95 ± 21 (8) *	41 ± 8 (6)*†

control Zucker lean (ZL-C); nebivolol ZL (ZL-N); control Zucker obese (ZO-C); nebivolol ZO (ZO-N). Data represent mean ± SE.

*P<0.05 vs ZL-C;

†P<0.05 vs ZO-C.

Table 2

Effects of nebivolol on *in vivo* cardiac functions in 8 week old ZL and ZO rats evaluated by cine-MRI.

Parameter	ZL-C	ZL-N	ZO-C	ZO-N
Cine MRI Data				
Sample Size	*10*	*6*	*10*	*6*
Age (weeks)	8.77 ± 0.09	8.14 ± 0.2	8.76 ± 0.09	8.07 ± 0.16
Heart Rate (bpm)	368 ± 7	383 ± 6	376 ± 10	363 ± 8
Stroke Volume (μL)	372.5 ± 20.1	314.8 ± 28	350.4 ± 19.2	303.7 ± 23.8
Ejection Fraction (%)	80.9 ± 1.5	75.6 ± 2.4	82.6 ± 1.9	80.2 ± 1.0
ED Septal Wall Thickness (mm)	1.41 ± 0.04	1.37 ± 0.03	1.78 ± 0.09 *	1.61 ± 0.04
Initial Filling Rate (μL/ms)	6.16 ± 0.49	5.67 ± 0.82	2.84 ± 0.58 *	3.88 ± 0.35
Peak Filling Rate (μL/ms)	8.07 ± 0.61	7.80 ± 0.91	8.61 ± 0.98	7.06 ± 0.51
Diastolic Relaxation (ms)	27.68 ± 2.50	27.50 ± 3.33	40.88 ± 1.95 *	32.77 ± 0.73 †

Data represent mean ± SE.

* P<0.05 vs ZL-C;

† P<0.05 vs ZO-C.